Available online at www.sciencedirect.com
SCIENCE DIRECT
International Journal of Heat and Mass Transfer 49 (2006) 2587–2596
International Journal of HEAT and MASS TRANSFER
www.elsevier.com/locate/ijhmt

Effect of fin thickness on the air-side performance of wavy fin-and-tube heat exchangers under dehumidifying conditions

Thirapat Kuvannarat [a], Chi-Chuan Wang [b], Somchai Wongwises [a,*]

[a] Department of Mechanical Engineering, Fluid Mechanics, Thermal Engineering and Multiphase Flow Research Lab (FUTURE), King Mongkut's University of Technology Thonburi, Bangmod, Bangkok 10140, Thailand
[b] Energy and Resources Laboratory, Industrial Technology Research Institute, Hsinchu 310, Taiwan, ROC

Received 11 July 2005; received in revised form 9 January 2006
Available online 20 March 2006

Abstract

This study investigated the effect of fin thickness on the air-side performance of wavy fin-and-tube heat exchangers under dehumidifying conditions. A total of 10 samples were tested with associated fin thickness (δ_f) of 0.115 mm and 0.25 mm, respectively. For a heat exchanger with two rows ($N = 2$) and fin pitch F_p of 1.41 mm, the effect of fin thickness on the heat transfer coefficient is more pronounced. The heat transfer coefficients for $\delta_f = 0.25$ mm is about 5–50% higher than those for $\delta_f = 0.115$ mm whereas the pressure drop for $\delta_f = 0.25$ mm is about 5–20% higher. The unexpected difference in heat transfer coefficient subject to fin thickness is attributable to better interactions between the directed main flow and the swirled flow caused by the condensate droplet for $\delta_f = 0.25$ mm. The maximum difference in heat transfer coefficients for $N = 2$ and $F_p = 2.54$ mm subject to the influence of fin thickness is reduced to about 20%, and there is no difference in heat transfer coefficient when the frontal velocity is above 3 m/s. For $N \geqslant 4$ and $F_p = 2.54$ mm, the influence of fin thickness on the heat transfer coefficients diminishes considerably. This is because of the presence of tube row, and the unsteady/vortex shedding feature at the down stream of wavy channel. Based on the present test results, a correlation is proposed to describe the air-side performance for wavy fin configurations, the mean deviations of the proposed heat transfer and friction correlations are 7.9% and 7.7%, respectively.

Keywords: Air-side performance; Wavy fin-and-tube heat exchangers; Colburn factor; Friction factor; Dehumidifying conditions

1. Introduction

Plate fin-and-tube heat exchangers are a basic type of heat exchanger employed in many industrial applications such as air conditioning, refrigeration and other thermal processes. In application, the dominated thermal resistance on the air-side of the heat exchanger normally limits the heat transfer rate. One way to enhance the heat transfer on the air-side of the heat exchanger is to modify the fin geometry. Among the enhanced fin configurations, herringbone wavy fin-and-tube heat exchangers are currently widely used because the corrugated fins can provide additional surface area and lengthen the mixing length of the airflow. In their application as evaporators, the surface temperature of the fins is generally below the dew point temperature. As a result, the moist air is condensed on the fins, giving rise to a significant change of the air-side performance of the heat exchanger. Development of the numerical simulation of fin-and-tube heat exchangers is generally difficult due to the complexity of the moist airflow pattern across the heat exchangers, so experimental study is needed.

The air-side performance of wavy fin-and-tube heat exchangers have been studied by a number of researches, see [1–5]. However, the effect of fin thickness on the air-side performance has received little attention in literature [6–8].

* Corresponding author. Tel.: +66 2 470 9115; fax: +66 2 470 9111.
E-mail address: somchai.won@kmutt.ac.th (S. Wongwises).

0017-9310/$ - see front matter © 2006 Elsevier Ltd. All rights reserved.
doi:10.1016/j.ijheatmasstransfer.2006.01.020

Nomenclature

A_f	surface area of fin, m^2
A_{min}	minimum free flow area, m^2
A_o	total surface area, m^2
$A_{p,i}$	inside surface area of tubes, m^2
$A_{p,o}$	outside surface area of tubes, m^2
b_p	slope of the air saturation curved between the outside and inside tube wall temperature, $J\,kg^{-1}\,K^{-1}$
b_r	slope of the air saturation curved at the mean water temperature and the inside wall temperature, $J\,kg^{-1}\,K^{-1}$
$b_{w,m}$	slope of the air saturation curved at the mean water film temperature of the fin surface, $J\,kg^{-1}\,K^{-1}$
$b_{w,p}$	slope of the air saturation curved at the mean water film temperature of the tube surface, $J\,kg^{-1}\,K^{-1}$
$C_{p,a}$	moist air specific heat at constant pressure, $J\,kg^{-1}\,K^{-1}$
$C_{p,w}$	water specific heat at constant pressure, $J\,kg^{-1}\,K^{-1}$
D_c	fin collar outside diameter, m
D_i	tube inside diameter, m
D_o	tube outside diameter, m
f	friction factor
f_i	in-tube friction factor
F	correction factor
F_p	fin pitch, mm
F_s	fin spacing, mm
G_{max}	mass flux of the air based on minimum free flow area, $kg\,m^{-2}\,s^{-1}$
h_{co}	sensible heat transfer coefficient, $W\,m^{-2}\,K^{-1}$
h_i	inside heat transfer coefficient, $W\,m^{-2}\,K^{-1}$
$h_{o,w}$	total heat transfer coefficient for wet external fin, $W\,m^{-2}\,K^{-1}$
I_0	modified Bessel function solution of the first kind, order 0
I_1	modified Bessel function solution of the first kind, order 1
$i_{a,in}$	inlet air enthalpy, $J\,kg^{-1}$
$i_{a,m}$	mean air enthalpy, $J\,kg^{-1}$
$i_{a,out}$	outlet air enthalpy, $J\,kg^{-1}$
i_m	mean enthalpy, $J\,kg^{-1}$
$i_{r,in}$	saturated air enthalpy at the inlet water temperature, $J\,kg^{-1}$
$i_{r,m}$	mean saturated air enthalpy at the mean water temperature, $J\,kg^{-1}$
$i_{r,out}$	saturated air enthalpy at the outlet water temperature, $J\,kg^{-1}$
$i_{s,fm}$	saturated air enthalpy at the fin mean temperature, $J\,kg^{-1}$
$i_{s,fb}$	saturated air enthalpy at the fin base temperature, $J\,kg^{-1}$
$i_{s,p,i,m}$	saturated air enthalpy at the mean inside tube wall temperature, $J\,kg^{-1}$
$i_{s,p,o,m}$	saturated air enthalpy at the mean outside tube wall temperature, $J\,kg^{-1}$
$i_{s,w,m}$	mean saturated air enthalpy at the mean water film temperature of the fin surface, $J\,kg^{-1}$
j	Colburn factor
K_0	modified Bessel function solution of the second kind, order 0
K_1	modified Bessel function solution of the second kind, order 1
K_c	contraction pressure loss coefficient
K_e	expansion pressure loss coefficient
k	thermal conductivity of fin, $W\,m^{-1}K^{-1}$
k_i	thermal conductivity of water, $W\,m^{-1}\,K^{-1}$
k_p	thermal conductivity of tube, $W\,m^{-1}\,K^{-1}$
k_w	thermal conductivity of water film, $W\,m^{-1}\,K^{-1}$
L	depth of heat exchanger, m
L_p	tube length, m
N	number of longitudinal tube rows
$\dot{m}_a$	air mass flow rate, $kg\,s^{-1}$
$\dot{m}_w$	water mass flow rate, $kg\,s^{-1}$
ΔP	pressure drop, Pa
P_L	longitudinal tube pitch, m
P_T	transverse tube pitch, m
P_d	wave height, m
Pr	Prandtl number
$\dot{Q}_a$	air-side heat transfer rate, W
$\dot{Q}_{avg}$	average heat transfer rate, W
$\dot{Q}_w$	water-side heat transfer rate, W
RH_{in}	inlet relative humidity
Re_{D_i}	Reynolds number based on inside diameter
Re_{D_c}	Reynolds number based on outside diameter (include collar)
r_i	distance from the center of the tube to the fin base, m
r_o	distance from the center of the tube to the fin tip, m
$T_{a,in}$	inlet air temperature, °C
$T_{p,i,m}$	mean temperature of the inner tube wall, °C
$T_{p,o,m}$	mean temperature of the outer tube wall, °C
$T_{r,m}$	mean temperature of water, °C
$T_{w,in}$	inlet water temperature, °C
$T_{w,out}$	outlet water temperature, °C
$U_{o,w}$	wet surface overall heat transfer coefficient, based on enthalpy difference, $kg\,m^{-2}\,s^{-1}$
V_c	maximum velocity across heat exchanger, $m\,s^{-1}$
V_{fr}	frontal velocity, $m\,s^{-1}$
y_w	thickness of condensate water film, m

Greek symbols

δ_f	fin thickness, m
$\eta_{f,wet}$	wet fin efficiency

θ	corrugation angle, degree	ρ_m	mean mass density of air, kg m^{-3}
ρ_i	mass density of inlet air, kg m^{-3}	σ	contraction ratio of cross-sectional area
ρ_o	mass density of outlet air, kg m^{-3}		

Recently, Wongwises and Chokeman [9] studied the effects of fin thickness on the heat transfer and friction characteristics of a fin-and-tube heat exchanger having herringbone wavy fin configuration under dry surface conditions. In contrast to a dry surface, there is no related data reported about the influence of fin thickness on the air-side performance when condensation takes place on the heat transfer surfaces. As a consequence, it is the main objective of this study to investigate the effects of fin thickness on the air-side heat transfer and friction characteristics of herringbone wavy fin-and-tube heat exchangers under dehumidifying conditions. Suitable correlations are also proposed to predict the heat transfer and friction characteristics.

2. Experimental apparatus

The schematic diagram of the experimental air-circuit assembly tunnel is shown in Fig. 1. It consists of a closed-loop wind tunnel in which air is circulated by an axial fan (2.2 kW), varying the air velocity with an inverter ranging 0.5–6 m/s. The air duct is made from galvanized steel sheet and has a 480 mm × 460 mm cross-section. To obtain a uniform flow into the tested channel, air was forced through a mixture and straightener before entering the test section. The airflow was measured by a nozzle based on the ASHRAE 41.2 Standard [10] and the pressure drops across the tested heat-exchanger and nozzle were detected by a manometer with uncertainty ±0.5 Pa. The inlet air temperature and humidity were controlled at approximately 28 °C and 60%, respectively. The inlet/outlet air temperatures across the test section and the inlet/outlet water temperatures from the tested heat exchanger were measured by T-type thermocouples having an accuracy of ±0.1 °C. The relative humidity across the tested heat-exchanger was controlled by a ventilation unit. A boiler was used to increase relative humidity. The working fluid in the tube-side of the heat exchanger was chilled water which provided a refrigeration system capacity of up to10.5 kW. The water temperature was kept constant at 7 °C; the water was pumped out of a storage tank, and was passed through a filter, flow meter, test section, and returned to the storage tank. The temperature differences on the water-side were measured by RTD (Pt-100 Ω), with a calibrated accuracy of ±0.05 °C. The flow rate of the water was kept constant at 0.14 kg/s and detected by a flow meter with a precision of ±0.01 kg/s.

A total of 10 herringbone wavy fin-and-tube heat exchangers, having various geometric parameters, were tested in this study. The details of the test samples are shown in Table 1. The accuracies of the measurement sensors and

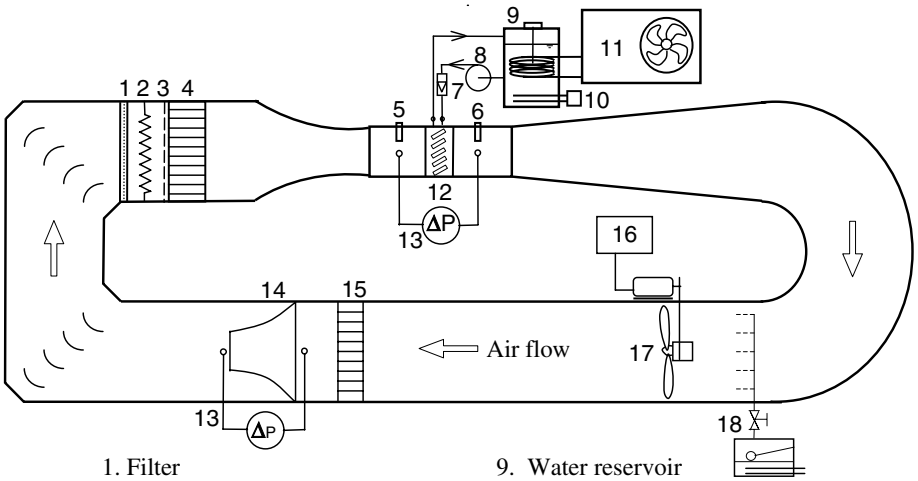

1. Filter
2. Air heater
3. Settling mean
4. Straightener
5. Inlet temperature and RH measuring section
6. Outlet temperature and RH measuring section
7. Water flow meter
8. Water pump
9. Water reservoir
10. Water heater
11. Chiller
12. Test heat exchanger
13. Manometer
14. Nozzle
15. Air mixer
16. Inverter
17. Axial fan
18. Humidifier

Fig. 1. Schematic diagram of the experimental apparatus.

Table 1
Geometric dimensions of the sample wavy fin-and-tube heat exchangers

No.	D_o (mm)	D_c (mm)	P_T (mm)	P_L (mm)	F_p (mm)	δ_f (mm)	N
1	9.53	9.76	25.4	19.05	1.41	0.115	2
2	9.53	9.76	25.4	19.05	1.81	0.115	2
3	9.53	9.76	25.4	19.05	2.54	0.115	2
4	9.53	9.76	25.4	19.05	2.54	0.115	4
5	9.53	9.76	25.4	19.05	2.54	0.115	6
6	9.53	10.03	25.4	19.05	1.41	0.250	2
7	9.53	10.03	25.4	19.05	1.81	0.250	2
8	9.53	10.03	25.4	19.05	2.54	0.250	2
9	9.53	10.03	25.4	19.05	2.54	0.250	4
10	9.53	10.03	25.4	19.05	2.54	0.250	6

Notes: Tube layouts of all heat exchangers are staggered layout. Tubes are made of copper with a wall thickness of 0.3 mm.

Table 2
The accuracies of the measurement

Parameters	Accuracy
Inlet air dry-bulb temperature, $T_{a,in}$	±0.1 °C
Inlet air relative humidity, RH_{in}	±5%
Pressure drop, ΔP	±0.5 Pa
Inlet water temperature, $T_{w,in}$	±0.1 °C
Water flow rate, $\dot{m}_w$	±0.01 kg/s

Table 3
Uncertainties of the derived experimental values

Parameters	Uncertainties (%)
Reynolds number, Re_{D_c}	±1.0
Air-side heat transfer rate, $\dot{Q}_a$	±5.5
Water-side heat transfer rate, $\dot{Q}_w$	±6.3
Pressure drop, ΔP	±0.5
Colburn factor, j	±15.4
Friction factor, f	±12.3

the uncertainties in derived experimental values are given in Tables 2 and 3. The geometrical parameters can be seen in Fig. 2. The geometric details of the tested herringbone wavy fins are shown in Fig. 3.

3. Data reduction

The following calculations are employed to determine the air-side heat transfer coefficient from the data recorded at steady state conditions during each test run. All fluid properties can be evaluated at the average temperature of the heat exchanger inlet and outlet. The method is based on Wang et al. [7] and Threlkeld [11]. The total rate of heat transfer is averaged from the air-side and water-side as follows:

$$\dot{Q}_a = \dot{m}_a(i_{a,in} - i_{a,out}) \tag{1}$$

$$\dot{Q}_w = \dot{m}_w C_{p,w}(T_{w,out} - T_{w,in}) \tag{2}$$

and

$$\dot{Q}_{avg} = (\dot{Q}_a + \dot{Q}_w)/2 \tag{3}$$

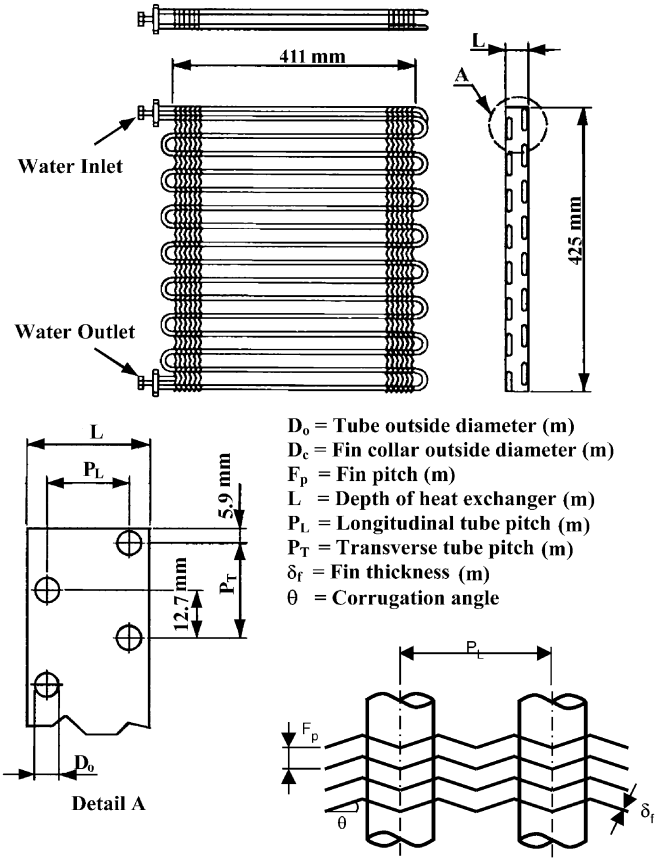

Fig. 2. Geometric details of the tested fin-and-tube heat exchangers, and water flow circuit inside the heat exchanger. (Dimension in mm.)

The overall heat transfer coefficient, $U_{o,w}$ which is based on the enthalpy potential can then be determined from

$$\dot{Q}_{avg} = U_{o,w}A_o F \Delta i_m \tag{4}$$

where A_o is the total surface area, F is the correction factor for the cross flow unmixed/unmixed configuration, and Δi_m is the mean enthalpy difference for the counter flow,

$$\Delta i_m = i_{a,m} - i_{r,m} \tag{5}$$

According to Myers [12], for the counter flow configuration, the mean enthalpy difference is

$$i_{a,m} = i_{a,in} + \frac{i_{a,in} - i_{a,out}}{\ln\left(\frac{i_{a,in} - i_{r,out}}{i_{a,out} - i_{r,in}}\right)} - \frac{(i_{a,in} - i_{a,out})(i_{a,in} - i_{r,out})}{(i_{a,in} - i_{r,out}) - (i_{a,out} - i_{r,in})} \tag{6}$$

$$i_{r,m} = i_{r,out} + \frac{i_{r,out} - i_{r,in}}{\ln\left(\frac{i_{a,in} - i_{r,out}}{i_{a,out} - i_{r,in}}\right)} - \frac{(i_{r,out} - i_{r,in})(i_{a,in} - i_{r,out})}{(i_{a,in} - i_{r,out}) - (i_{a,out} - i_{r,in})} \tag{7}$$

The overall heat transfer coefficient can be written in terms of the total resistance to heat transfer. This total resistance is the sum of the individual resistance as follows:

$$\frac{1}{U_{o,w}} = \frac{b_r A_o}{h_i A_{p,i}} + \frac{b_p A_o \ln\left(\frac{D_c}{D_i}\right)}{2\pi k_p L_p} + \frac{1}{h_{o,w}\left(\frac{A_{p,o}}{b_{w,p}A_o} + \frac{A_f \eta_{f,wet}}{b_{w,m}A_o}\right)} \tag{8}$$

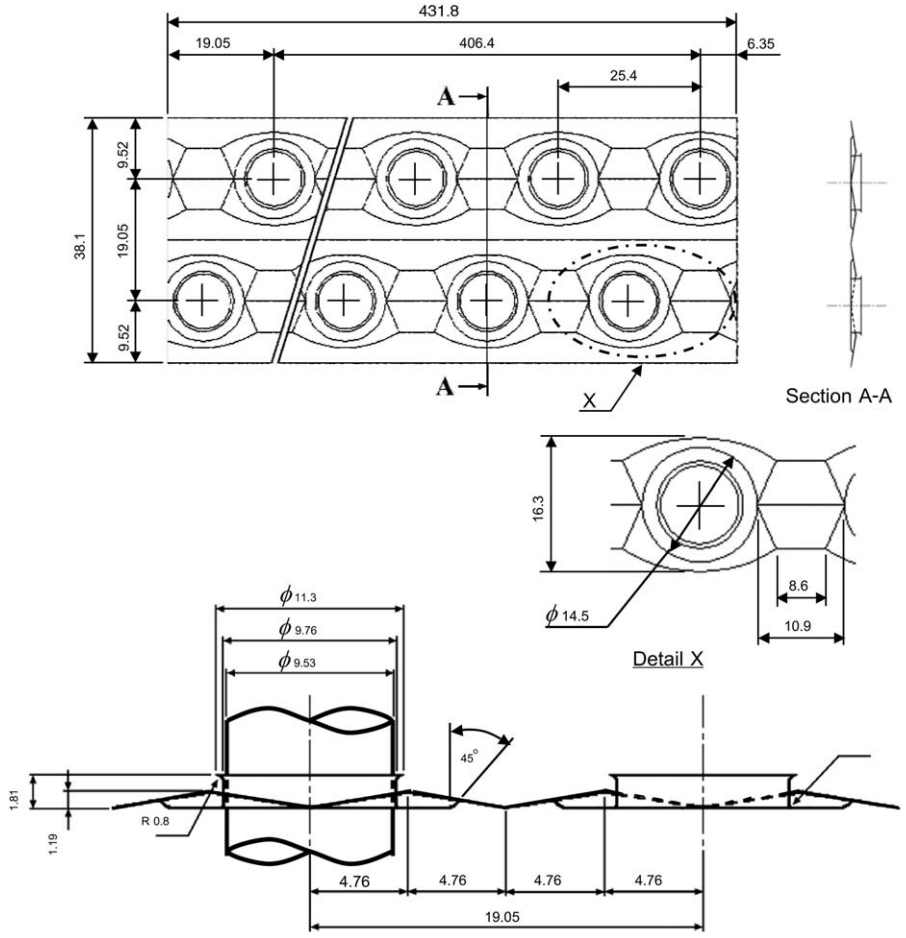

Fig. 3. Geometric details of the tested herringbone wavy fins. (Dimension in mm.)

where

$$h_{o,w} = \frac{1}{\frac{C_{p,a}}{b_{w,m}h_{co}} + \frac{y_w}{k_w}} \tag{9}$$

where y_w is the water film thickness. In general practice, the value of y_w/k_w is only 0.5–5% compared to $C_{p,a}/b_{w,m}h_{co}$ [7]. This term is therefore neglected.

The tube-side heat transfer coefficient, (h_i), is evaluated from the semi-empirical correlation of Gnielinski [13]:

$$h_i = \frac{k_i}{D_i} \cdot \frac{(Re_{D_i} - 1000)Pr(f_i/2)}{1 + 12.7\sqrt{f_i/2}(Pr^{2/3} - 1)} \tag{10}$$

where the friction factor is given by

$$f_i = \frac{1}{(1.58 \ln Re_{D_i} - 3.28)^2} \tag{11}$$

The values of b_r and b_p can be determined from

$$b_r = \frac{(i_{s,p,i,m} - i_{r,m})}{(T_{p,i,m} - T_{r,m})} \tag{12}$$

$$b_p = \frac{(i_{s,p,o,m} - i_{s,p,i,m})}{(T_{p,o,m} - T_{p,i,m})} \tag{13}$$

The values of $b_{w,p}$ and $b_{w,m}$ are slopes of the saturated enthalpy curve evaluated at the base surface and the fin surface at the outer mean water film temperature. The value of $b_{w,m}$ is determined by trial and error. For the trial and error procedure, the following equation is used to determine $i_{s,w,m}$

$$i_{s,w,m} = i_{a,m} - \frac{C_{p,a}h_{o,w}\eta_{f,wet}}{b_{w,m}h_{co}} \times \left(1 - U_{o,w}A_o\left[\frac{b_r}{h_iA_{p,i}} + \frac{b_p \ln\left(\frac{D_e}{D_i}\right)}{2\pi k_p L_p}\right]\right) \times (i_{a,m} - i_{r,m}) \tag{14}$$

The wet fin efficiency, $\eta_{f,wet}$ can be determined based on the Wang [7] method as follows:

$$\eta_{f,wet} = \frac{2r_i}{M_T(r_o^2 - r_i^2)}\left[\frac{K_1(M_Tr_i)I_1(M_Tr_o) - K_1(M_Tr_o)I_1(M_Tr_i)}{K_1(M_Tr_o)I_o(M_Tr_i) + K_o(M_Tr_i)I_1(M_Tr_o)}\right] = \frac{i_{a,m} - i_{s,fm}}{i_{a,m} - i_{s,fb}} \tag{15}$$

where $M_T = \sqrt{\frac{2h_{o,w}}{k\delta}}$ and $r_o = \sqrt{\frac{P_TP_L}{\pi}}$.

The air-side heat transfer characteristics are presented in terms of the Colburn j factor

$$j = \frac{h_{c,o}}{G_{max}C_{p,a}}Pr^{2/3} \tag{16}$$

The flow characteristics determined from the equation proposed by Kays and London [14] termed as the Fanning friction factor. The equation includes the entrance and exit pressure losses:

$$f = \frac{\rho_m A_{min}}{\rho_i A_o}\left[\frac{2\rho_i \Delta P}{G_{max}^2} - (1-\sigma^2+K_c) - 2\left(\frac{\rho_i}{\rho_o}-1\right) + (1-\sigma^2-K_e)\frac{\rho_i}{\rho_o}\right] \quad (17)$$

where $G_{max} = \rho_m V_c$ and V_c is the maximum velocity in the heat exchanger core. σ is the ratio of the minimum free flow area to the frontal area, A_o is the total heat transfer area, A_{min} is the minimum free flow area, K_c is the core entrance loss coefficient (sudden contraction) and K_e is the exit loss (sudden enlargement) coefficient.

4. Results and discussion

The air-side heat transfer and friction characteristics of all tested samples were determined from the experimental data. The thicknesses of the herringbone wavy fins examined in this study were 0.115 and 0.250 mm. The heat transfer coefficient and air-side pressure drop were plotted against the frontal velocity for the tested samples 1 and 6, as shown in Fig. 4. As can be seen in Fig. 4, it was found that the heat transfer coefficient and pressure drop increase with frontal velocity. For Fig. 4(a), the corresponding fin pitch of these two samples is 1.41 mm. Hence, the effective fin spacing for $\delta_f = 0.25$ and $\delta_f = 0.115$ mm is 1.16 mm and 1.3 mm, respectively. The difference between the fin spacing is about 11%. However, it is interested to note that the heat transfer coefficients for $\delta_f = 0.25$ mm are about 5–50% higher than those of $\delta_f = 0.115$ mm whereas the pressure drop of the thick fin is higher than of the thin fin for around 5–20%. The difference is generally increased with the rise of frontal velocities. The surprising differences in heat transfer coefficient between larger and smaller fin thickness are in connection with the drop size and airflow pattern. As indicated by Lin et al. [8,15] who respectively performed a flow visualization of condensate flow patterns along plate surface fin and herringbone fin surface, they reported that the drop size of the condensate is in the range of 0.1–0.5 mm with a corresponding drop height in the range of 0.1–0.7 mm. The presence of condensate is on both sides of the fin. In that regard, the condensate acts not only like a roughness but also a vortex generator. This phenomenon is especially reinforced when the drop size is comparable to the fin spacing. The explanation can be further made clear from the flow visualization experiments conducted by Yoshii et al. [16] who tested a scale-up model of a herringbone fin-and-tube heat exchanger under dehumidifying condition. Yoshii et al. [16] noticed that when the fin channel is close to each other, the condensate which adheres to both sides may cause the airflow within the channel to twist. As a consequence, one can see a dramatic

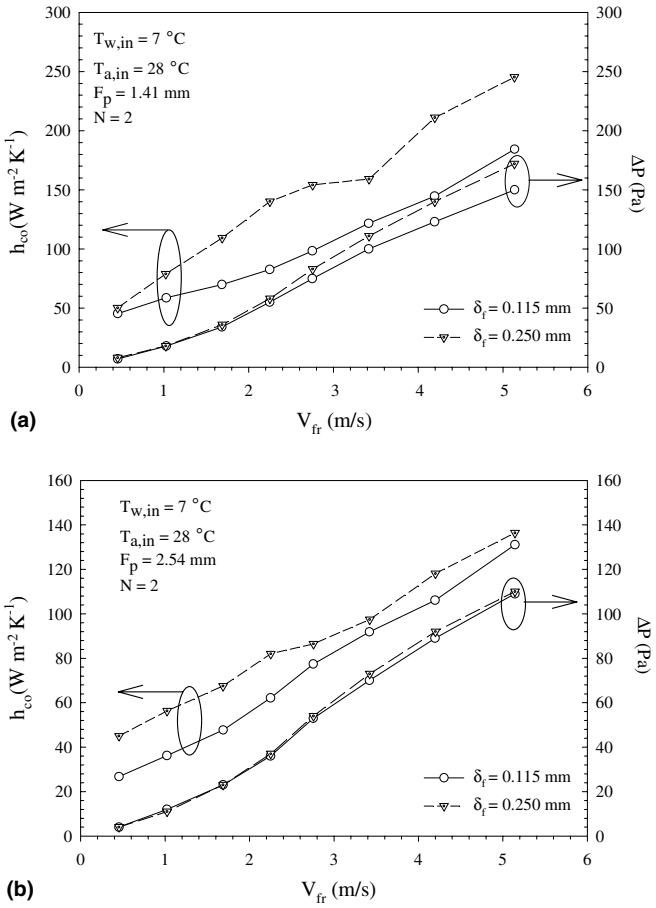

Fig. 4. Effect of fin thickness on the heat transfer coefficient and pressure drop for 2-row configuration: test results for (a) $F_p = 1.41$ mm and (b) $F_p = 2.54$ mm.

rise of heat transfer coefficient due to the presence of swirled flow when the channel distance is reduced.

For the same number of tube row ($N = 2$), one can see the associated influence of fin thickness on the heat transfer coefficient is decreased when the fin pitch is increased to 2.54 mm as seen in Fig. 4(b). In fact the maximum difference in heat transfer coefficients subject to the influence of fin thickness is reduced to about 50%, and one can see there is no difference in heat transfer coefficient when the frontal velocity is above 3 m/s. A detailed explanation of the test results will be made in the following paragraph.

A schematic showing the influence of fin thickness in corrugated channels for a smaller and larger fin spacing is shown in Fig. 5. Apparently the airflow may interact with the condensate droplet, giving way to swirled motions. For a larger fin thickness, the corresponding fin spacing is comparatively small. As a consequence, the generated swirled flow may mingle with the main flow and result in a higher heat transfer performance. This phenomenon becomes more pronounced with the frontal velocities which agree well with the trend shown in Fig. 4. Conversely, as shown in Fig. 5b, the interactions between the generated swirled motions and main flow is less prominent at a smaller fin thickness in which the fin spacing is larger. Note that

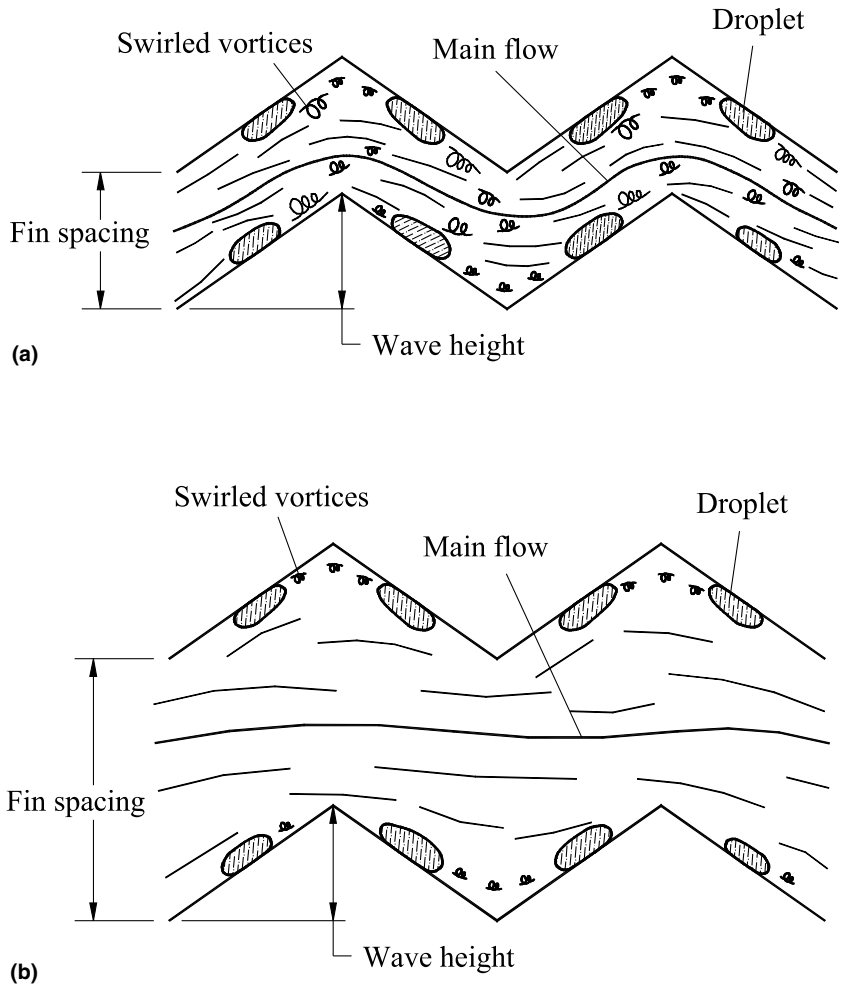

Fig. 5. Schematic showing the interactions between directed airflow and generated swirled flow for small and large fin spacing: (a) smaller fin spacing and (b) larger fin spacing.

the presented schematic in Fig. 5 also reveals a special characteristic that deserve further attentions. As seen in Fig. 5b, for a larger fin spacing, the main flow may not be effectively directed by the corrugated channel whereas the main flow can flow along the corrugated channel more effectively provided that the fin spacing is less than wave height ($F_s < P_d$). This phenomenon had been confirmed by a numerical visualization of the flow pattern within corrugated channels from McNab et al. [17]. Analogous results were also reported by Wang et al. [18] who conducted a flow visualization experiment within enlarged corrugated channels. By examination of the details of the present herringbone fin configurations as shown in Fig. 3, one can see the corresponding wave height is 1.19 mm. As a consequence, for a larger fin thickness of $\delta_f = 0.25$ mm, the relevant fin spacing is 1.13 mm which is smaller than the wave height. This suggests the airflow is effectively directed by the corrugations. In the meantime, at a smaller fin thickness of $\delta_f = 0.115$ mm, the associated fin spacing is 1.3 mm that is larger than the wave height. Some part of the airflow is prone to flow across the corrugation without directing by the wave height. As a result, one can see a dramatic difference of heat transfer coefficient between $\delta_f = 0.25$ and $\delta_f = 0.115$ mm. Based on foregoing explanation of the schematic of Fig. 5, one can clearly understand the difference between test results of Fig. 4(a) and (b).

The aforementioned results are applicable for $N = 2$ where corrugations of the wavy channels is comparatively small. With the increase of fin spacing and the number of tube rows, the associated influence of fin thickness on the heat transfer coefficients will be reduced. We will defer this explanations after checking the test results of $N = 4$ and 6 as shown in Fig. 6. The test results in Fig. 6 clearly substantiate the general arguments made. As seen in Fig. 6(a), despite the heat transfer coefficients for $\delta_f = 0.25$ mm are higher than those of $\delta_f = 0.115$ mm for $N = 4$ and $F_p = 2.54$ mm, the difference is within 15%. Moreover, one can see that there is barely no difference in heat transfer coefficients and pressure drops between $\delta_f = 0.25$ mm and $\delta_f = 0.115$ mm for $N = 6$ and $F_p = 2.54$ mm. There are two major explanations about the diminishing influence of fin thickness at a larger fin spacing and at a larger number of tube rows. The first one is related to the influence of tube row. The presence of tube row will certainly alter the airflow

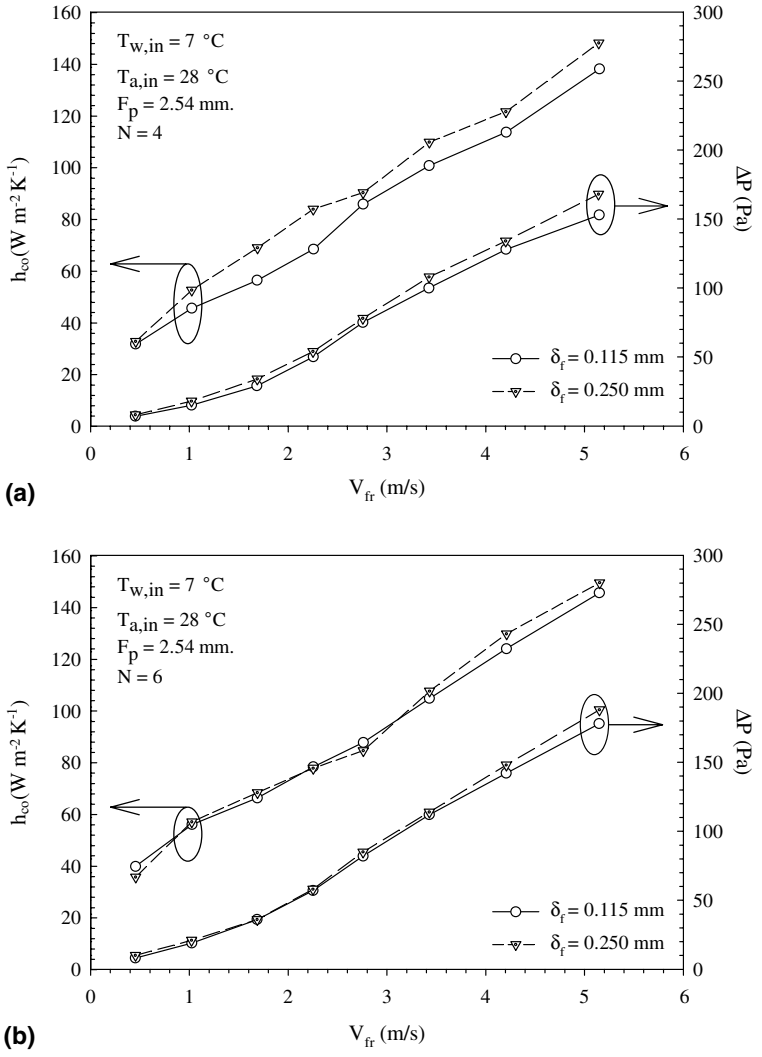

Fig. 6. Effect of fin thickness on the heat transfer coefficient and pressure drops: test results for (a) samples 4 and 9 having 4-row configuration and a fin pitch of 2.54 mm; (b) samples 5 and 10 having 6-row configuration and a fin pitch of 2.54 mm.

path and induces horseshoe vortices [19] that will mix with the main flow. Furthermore, as mentioned in preceding section, the main airflow will interact with the swirled flow caused by the condensate. The presence of tube row will alter the airflow direction, resulting in better flow mixing. The second and most influential reason may be attributed to the nature of wave channels. As can be seen from Ali and Ramadyani [20] who performed a flow visualization experiment in two wavy channels using a dye tracking technique, the fluid flow in the first few corrugations is laminar. However, depending on the Reynolds number, spanwise vortices were shed periodically from certain corrugation at the downstream of a wider channel, but vortex shedding was not observed in narrow channel. Their flow visualization shows considerable flow mixing after several corrugations provided that the fin spacing is large. Wang et al. [18] also observed a unsteady swing at the downstream of a wavy channel that will also promote (or enhance) flow mixing. This apparently agrees with the larger number of tube rows and larger fin spacing of the test results of Fig. 6. In essence, pronounced mixing occurred at a larger fin spacing and at a larger number of tube row, the influence of fin thickness or condensate on the airflow mixing is therefore rather small. Also from Fig. 6, it is also found that the fin thickness has a negligible effect on the friction characteristic when the number of tube rows $N \geqslant 4$. This is again related to the significant mixing of airflow pattern.

It is obvious from the test results from previous discussions that no single curve can be expected to describe the complex behavior of the present wavy fin for both heat transfer and frictional characteristics. Thus, a multi-regression is carried out to obtain the appropriate correlation form of j and f for the present wavy fin configuration. It is recommended that the following equations are used to describe the present j and f.

$$j = 0.213262 Re_{D_c}^{-0.51507} N^{0.09891} \left(\frac{A_o}{A_{p,o}}\right)^{0.600543} \left(\frac{\delta_f}{P_L}\right)^{0.072448} \quad (18)$$

$$f = 64.0542 Re_{D_c}^{-0.69284} N^{-0.5237} \left(\frac{A_o}{A_{p,o}}\right)^{-0.54736} \left(\frac{\delta_f}{P_L}\right)^{-0.98371} \quad (19)$$

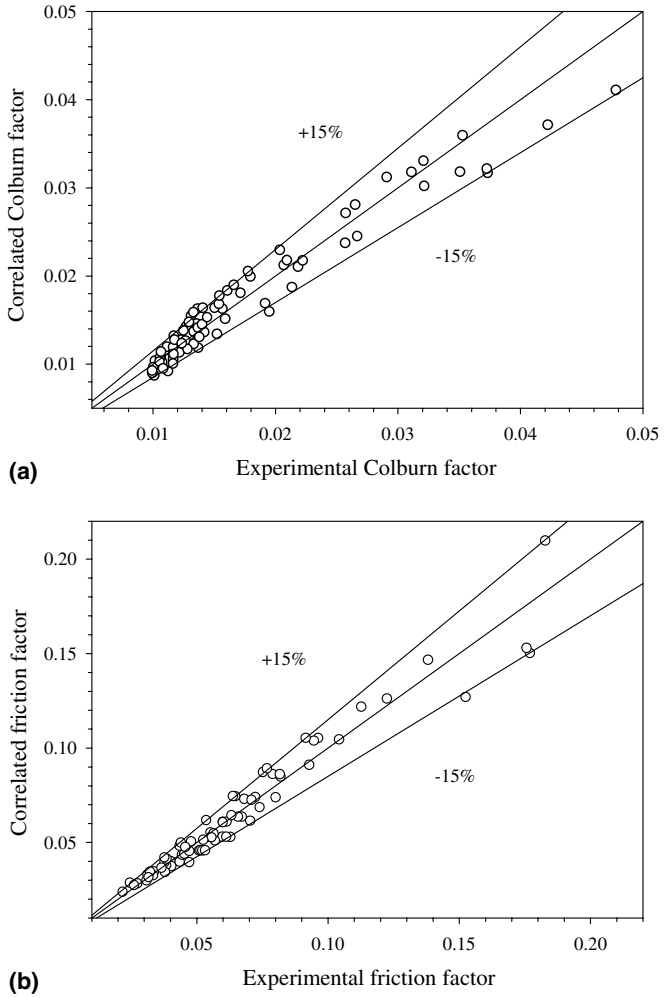

Fig. 7. Comparison of the proposed correlations against experimental data: (a) Colburn j factor and (b) friction factor.

As shown in Fig. 7, the proposed heat transfer and friction correlations (Eqs. (18) and (19)) can describe 91.3% and 87.5% of the j and f factors within ±15%, respectively. The mean deviations of the proposed heat transfer and friction correlations are 7.9% and 7.7%, respectively.

5. Conclusions

The present study investigated the effect of fin thickness on the air-side performance of wavy fin-and-tube heat exchangers under dehumidifying conditions. A total of 10 samples were tested with associated fin thickness of 0.115 mm and 0.25 mm, respectively. The following conclusions based on the test results can be made:

1. For $N = 2$ and $F_p = 1.41$ mm, the effect of fin thickness on the heat transfer coefficient is more pronounced. The heat transfer coefficients for $\delta_f = 0.25$ mm is about 5–50% higher than those for $\delta_f = 0.115$ mm whereas the pressure drop for $\delta_f = 0.25$ mm is about 5–20% higher. The unexpected difference in heat transfer coefficient subject to fin thickness is attributable to better interactions between the directed main flow and the swirled flow caused by the condensate droplet for $\delta_f = 0.25$ mm.
2. For $N = 2$ and $F_p = 2.54$ mm, the associated influence of fin thickness on the heat transfer coefficient is decreased when compared to those of $F_p = 1.41$ mm. The maximum difference in heat transfer coefficients subject to the influence of fin thickness is reduced to approximately 20%, and there is no difference in heat transfer coefficient when the frontal velocity is above 3 m/s.
3. For $N \geqslant 4$ and $F_p = 2.54$ mm, the influence of fin thickness on the heat transfer coefficients diminishes considerably. There is negligible difference for $N = 6$. This is due to the presence of tube row, and the unsteady/vortex shedding feature at the down stream of wavy channel that lead to a significant mixing. Analogous results about the influence of fin thickness on the pressure drop is also shown.
4. Based on the present test results, a correlation is proposed to describe the air-side performance for wavy fin configurations, it is found that 91.3% of the j factors and 87.5% of the friction factors within ±15%. The mean deviations of the proposed heat transfer and friction correlations are 7.9% and 7.7%, respectively.

Acknowledgements

The present study was financially supported by the Thailand Research Fund (TRF) and Joint Graduate School of Energy and Environment (JGSEE) whose guidance and assistance are gratefully acknowledged. The second author wishes to acknowledge the financial supports provided by the Energy Bureau of the Ministry of Economic Affairs, Taiwan, ROC.

References

[1] D.T. Beecher, T.J. Fagan, Effects of fin pattern on the air-side heat transfer coefficient in plate finned-tube heat exchanger, ASHRAE Trans. 93 (2) (1987) 1961–1984.
[2] C.C. Wang, W.L. Fu, C.T. Chang, Heat transfer and friction characteristics of typical wavy fin-and-tube heat exchangers, Exp. Thermal Fluid Sci. 14 (1997) 174–186.
[3] C.C. Wang, Y.M. Tsi, D.C. Lu, A comprehensive study of convex-louver and wavy fin-and-tube heat exchangers, AIAA J. Thermophys. Heat Transfer 12 (1998) 423–430.
[4] C.C. Wang, Y.T. Lin, C.J. Lee, Investigation of wavy fin-and tube heat exchangers: a contribution to databank, Exp. Heat Transfer 12 (1999) 73–89.
[5] W.M. Yan, P.J. Sheen, Heat transfer and friction characteristic of fin-and tube heat exchangers, Int. J. Heat Mass Transfer 43 (2000) 1651–1659.
[6] C.C. Wang, Y.J. Chang, Y.C. Hsieh, Y.T. Lin, Sensible heat and friction characteristics of plate fin-and-tube heat exchangers having plane fins, Int. J. Refrig. 19 (4) (1996) 223–230.
[7] C.C. Wang, Y.C. Hsieh, Y.T. Lin, Performance of plate finned tube heat exchangers under dehumidifying conditions, ASME J. Heat Transfer 119 (1997) 109–117.

[8] Y.T. Lin, Y.M. Hwang, C.C. Wang, Performance of the herringbone wavy fin under dehumidifying conditions, Int. J. Heat Mass Transfer 45 (2002) 5035–5044.
[9] S. Wongwises, Y. Chokeman, Effect of fin thickness on air-side performance of herringbone wavy fin-and-tube heat exchangers, Heat Mass Transfer 41 (2004) 147–154.
[10] ASHRAE Standard 41.2, Standard Methods for Laboratory Air-Flow Measurement, American Society of Heating, Refrigerating and Air-Conditioning Engineering, Atlanta, 1987.
[11] J.L. Threlkeld, Thermal Environmental Engineering, Prentice-Hall, New York, 1970.
[12] R.J. Myers, The effect of dehumidification on the air-side heat transfer coefficient for a finned-tube coil, MS Thesis, University of Minnesota, Minneapolis, 1967.
[13] V. Gnielinski, New equation for heat and mass transfer in turbulent pipe and channel flow, Int. Chem. Eng. 16 (1976) 359–368.
[14] W.M. Kays, A. London, Compact Heat Exchangers, third ed., McGraw-Hill, New York, 1984.
[15] Y.T. Lin, K.C. Hsu, Y.J. Chang, C.C. Wang, Performance of rectangular fin in wet conditions: visualization and wet fin efficiency, ASME J. Heat Transfer 123 (2001) 827–836.
[16] T. Yoshii, M. Yamamoto, T. Otaki, Effects of dropwise condensate on wet surface heat transfer of air cooling coils, in: Proceedings of the 13th International Congress of Refrigeration, International Institute of Refrigeration, Paris, 1973, pp. 285–292.
[17] C.A. McNab, K.N. Atkinson, M.R. Heikal, Numerical modeling of heat transfer and fluid flow over herringbone corrugated fins, Heat Transfer 6 (1998) 119–124.
[18] C.C. Wang, M.T. Hung, R.H. Yeh, Y.J. Chang, S.P. Liaw, Flow visualization inside the wavy channels, Int. J. Heat Exch 5 (2004) 1–13.
[19] C.C. Wang, J. Lo, Y.T. Lin, C.S. Wei, Flow visualization of annular and delta winglet vortex generators in fin-and-tube heat exchanger application, Int. J. Heat Mass Transfer 45 (18) (2002) 3803–3815.
[20] M.M. Ali, S. Ramadyani, Experiments on convective heat transfer in corrugated channels, Exp. Heat Transfer 5 (1992) 175–193.